Available online at www.sciencedirect.com

ScienceDirect

Nuclear Physics B 888 (2014) 169–193

NUCLEAR PHYSICS B

www.elsevier.com/locate/nuclphysb

Measurement of *CP* violation and constraints on the CKM angle γ in $B^{\pm} \to DK^{\pm}$ with $D \to K^0_S\pi^+\pi^-$ decays

LHCb Collaboration

Received 24 July 2014; received in revised form 8 September 2014; accepted 19 September 2014

Available online 28 September 2014

Editor: Tommy Ohlsson

Abstract

A model-dependent amplitude analysis of $B^{\pm} \to DK^{\pm}$ with $D \to K^0_S\pi^+\pi^-$ decays is performed using proton–proton collision data, corresponding to an integrated luminosity of 1 fb^{-1}, recorded by LHCb at a centre-of-mass energy of 7 TeV in 2011. Values of the *CP* violation observables $x_{\pm}$ and $y_{\pm}$, which are sensitive to the CKM angle γ, are measured to be

$$x_- = +0.027 \pm 0.044^{+0.010}_{-0.008} \pm 0.001,$$
$$y_- = +0.013 \pm 0.048^{+0.009}_{-0.007} \pm 0.003,$$
$$x_+ = -0.084 \pm 0.045 \pm 0.009 \pm 0.005,$$
$$y_+ = -0.032 \pm 0.048^{+0.010}_{-0.009} \pm 0.008,$$

where the first uncertainty is statistical, the second systematic and the third arises from the uncertainty of the $D \to K^0_S\pi^+\pi^-$ amplitude model. The value of γ is determined to be $(84^{+49}_{-42})^\circ$, including all sources of uncertainty. Neutral D meson mixing is found to have negligible effect.

1. Introduction

The CKM phase γ ($\gamma \equiv \arg[-V_{ud}V^*_{ub}/V_{cd}V^*_{cb}]$, also known as ϕ_3) is the angle of the CKM unitarity triangle that is least constrained by direct measurements. The precise determination of

http://dx.doi.org/10.1016/j.nuclphysb.2014.09.015

γ is an important aim of current flavour physics experiments. It can be measured directly in tree-level processes, for example in $B^{\pm} \to DK^{\pm}$ decays where D is a superposition of the flavour eigenstates D^0 and $\overline{D}^0$ decaying into the same final state. Sensitivity to γ arises from the interference between $b \to u$ and $b \to c$ quark transitions. Since $B^{\pm} \to DK^{\pm}$ decays are expected to be insensitive to physics processes beyond the Standard Model (SM), this measurement provides a reference value against which other observables, potentially affected by physics beyond the SM, can be compared.

The determination of γ (using $B^{\pm} \to DK^{\pm}$ decays) from an amplitude analysis of the D meson decay to the three-body quasi-self-conjugate $K^0_S\pi^+\pi^-$ final state was first proposed in Refs. [1,2]. The method requires knowledge of the $D \to K^0_S\pi^+\pi^-$ decay amplitude across the phase space and, in particular, its strong phase variation. The model-dependent approach, as used in Refs. [3–8], implements a model to describe the D decay amplitude over the phase space. This unbinned method allows for full exploitation of the statistical power of the data. A model-independent strategy, employed by the LHCb [9] and Belle [10] Collaborations, uses CLEO measurements [11] of the D decay strong phase difference in bins across the phase space.

Neglecting the effects of charm mixing, the amplitude for $B^{\pm} \to D(\to K^0_S\pi^+\pi^-)K^{\pm}$ decays can be written as a superposition of Cabibbo favoured and suppressed contributions,

$$\begin{aligned} \mathcal{A}_{B^-} &\sim A_f + r_B e^{i(\delta_B - \gamma)} \bar{A}_f, \\ \mathcal{A}_{B^+} &\sim \bar{A}_f + r_B e^{i(\delta_B + \gamma)} A_f, \end{aligned} \tag{1}$$

where r_B is the magnitude of the ratio of the interfering $B^{\pm}$ decay amplitudes, δ_B is the strong phase difference between them, and γ is the CP-violating weak phase. The amplitudes of the D^0 and $\overline{D}^0$ mesons decaying into the common final state f, $A_f \equiv \langle f|\mathcal{H}|D^0\rangle$ and $\bar{A}_f \equiv \langle f|\mathcal{H}|\overline{D}^0\rangle$, respectively, depend on two squared invariant masses of pairs of the three final state particles, chosen to be $m^2_+ \equiv m^2_{K^0_S\pi^+}$ and $m^2_- \equiv m^2_{K^0_S\pi^-}$. Assuming that no direct CP violation exists in the D meson decay, the amplitudes A_f and $\bar{A}_f$ are related by $\bar{A}_f(m^2_+, m^2_-) = A_f(m^2_-, m^2_+)$. A direct determination of r_B, δ_B and γ can lead to bias [3], and hence the Cartesian CP violation observables, $x_{\pm} = r_B \cos(\delta_B \pm \gamma)$ and $y_{\pm} = r_B \sin(\delta_B \pm \gamma)$, are used, where the "+" and "–" indices correspond to B^+ and B^- decays, respectively.

This paper reports measurements of $(x_{\pm}, y_{\pm})$ made using $B^{\pm} \to D(\to K^0_S\pi^+\pi^-)K^{\pm}$ decays selected from pp collision data, corresponding to an integrated luminosity of 1 fb^{-1}, recorded by LHCb at a centre-of-mass energy of 7 TeV in 2011. The data set is identical to that used in Ref. [9]. The measured values of $(x_{\pm}, y_{\pm})$ place constraints on the CKM angle γ.

2. The LHCb detector

The LHCb detector [12] is a single-arm forward spectrometer covering the pseudorapidity range $2 < \eta < 5$, designed for the study of particles containing b or c quarks. The detector includes a high-precision tracking system consisting of a silicon-strip vertex detector surrounding the pp interaction region, a large-area silicon-strip detector located upstream of a dipole magnet with a bending power of about 4 Tm, and three stations of silicon-strip detectors and straw drift tubes placed downstream of the magnet. The combined tracking system provides a momentum measurement with a relative uncertainty that varies from 0.4% at low momentum, p, to 0.6% at 100 GeV/c, and an impact parameter measurement with a resolution of 20 μm for charged particles with large transverse momentum, p_{T}. Different types of charged hadrons are distinguished

using information from two ring-imaging Cherenkov detectors [13], providing particle identification (PID) information. Photon, electron and hadron candidates are identified by a calorimeter system consisting of scintillating-pad and preshower detectors, an electromagnetic calorimeter and a hadronic calorimeter. Muons are identified by a system composed of alternating layers of iron and multiwire proportional chambers.

The trigger consists of a hardware stage, based on information from the calorimeter and muon systems, followed by a software stage, which applies a full event reconstruction. The software trigger requires a two-, three- or four-track secondary vertex with a large sum p_{T} of the tracks and a significant displacement from any primary pp interaction vertex (PV). At least one track should also have large p_{T} and χ^2_{IP} with respect to any primary interaction, where χ^2_{IP} is defined as the difference in χ^2 of a given PV reconstructed with and without the considered track. A multivariate algorithm [14] is used to identify secondary vertices consistent with decays of b hadrons.

Large samples of simulated $B^\pm \to D(\to K^0_{\mathrm{S}}\pi^+\pi^-)K^\pm$ and $B^\pm \to D(\to K^0_{\mathrm{S}}\pi^+\pi^-)\pi^\pm$ decays are used in this study, along with simulated samples of various background decays. In the simulation, pp collisions are generated using PYTHIA 6.4 [15] with a specific LHCb configuration [16]. Decays of hadronic particles are described by EVTGEN [17], in which final state radiation is generated using PHOTOS [18]. The interaction of the generated particles with the detector and its response are implemented using the GEANT4 toolkit [19,20] as described in Ref. [21].

3. Candidate selection and sources of background

The criteria used to select $B^\pm \to D(\to K^0_{\mathrm{S}}\pi^+\pi^-)K^\pm$ and $B^\pm \to D(\to K^0_{\mathrm{S}}\pi^+\pi^-)\pi^\pm$ candidate decays from the data are described below. The $B^\pm \to D(\to K^0_{\mathrm{S}}\pi^+\pi^-)\pi^\pm$ decays are used to measure the acceptance over phase space, as they have almost identical topologies to $B^\pm \to D(\to K^0_{\mathrm{S}}\pi^+\pi^-)K^\pm$ decays, but a much higher branching fraction [22]. Apart from the $B^\pm$ candidate invariant mass range, the selection requirements are identical to those used in Ref. [9] and are summarised here for completeness.

Candidate K^0_{S} mesons are reconstructed from two oppositely charged well-measured tracks; those with tracks reconstructed in the silicon vertex detector are known as *long* candidates and those with tracks that cannot be formed in the vertex detector are known as *downstream* candidates. A requirement of χ^2_{IP} greater than 16 (4) with respect to the PV is made for the *long* (*downstream*) pion tracks. The PV of each candidate $B^\pm$ meson decay is chosen to be the one yielding the minimum χ^2_{IP}. To reduce background from random track combinations, the cosine of the angle between the momentum direction of the K^0_{S} meson candidate and the direction vector from the PV to its decay vertex is required to be greater than 0.99.

The K^0_{S} candidates are combined with two oppositely charged tracks to reconstruct D meson candidates; the tracks combined with a *long* (*downstream*) candidate must have χ^2_{IP} greater than 9 (16) with respect to the PV. For all D meson candidates, requirements of χ^2_{IP} greater than 9 with respect to the PV and cosine of the angle between the momentum and direction vectors greater than 0.99 are made. It is required that the vertex separation χ^2 between the reconstructed D and K^0_{S} meson decay vertices is greater than 100, where the vertex separation χ^2 is defined as the change in χ^2 of a vertex which is reconstructed including the particles originally contributing to the other vertex. The reconstructed D meson candidate invariant mass is required to be within ± 25 MeV/c^2 around the known value [22]. The K^0_{S} candidate invariant mass must be within ± 15 MeV/c^2 around the known value [22] after a refit to constrain the D meson mass [23].

The $B^\pm$ meson candidates are reconstructed from the combination of a D meson candidate with a pion or kaon directly from the $B^\pm$ vertex, hereafter called the "bachelor" track. The bachelor track is required to have $\chi^2_{\rm IP}$ greater than 25 with respect to the PV. To separate $B^\pm \to DK^\pm$ and $B^\pm \to D\pi^\pm$ decays, good discrimination between pions and kaons is required using PID information. The $\chi^2_{\rm IP}$ of the reconstructed $B^\pm$ candidate with respect to the PV is required to be less than 9, and for *long* (*downstream*) candidates the cosine of the angle between its momentum and direction vectors must be greater than 0.9999 (0.99995). The $B^\pm$ vertex separation χ^2 with respect to the PV must be greater than 169. In addition, the reconstructed D meson decay vertex is required to have a larger longitudinal displacement from the PV than the $B^\pm$ decay vertex.

Each selected candidate decay is refitted with additional constraints on the K^0_S and D meson masses and on the pointing of the B momentum to the PV, so that improved resolution in the phase space of the D decay is obtained. A refit quality requirement of χ^2 per degree of freedom less than 5 is made. If more than one selected candidate is found to originate from the same pp collision event, the candidate with the lowest value of refit χ^2 per degree of freedom is retained.

Several sources of potential background are studied using simulation. These include two categories of combinatorial background: a real $D \to K^0_S\pi^+\pi^-$ decay combined with a random bachelor track (random Dh), or a $D \to K^0_S\pi^+\pi^-$ candidate reconstructed with at least one random final state track (combinatorial D). Cross-feed background arises from $B^\pm \to D(\to K^0_S\pi^+\pi^-)\pi^\pm$ decays misidentified as $B^\pm \to D(\to K^0_S\pi^+\pi^-)K^\pm$ decays (or vice versa), and contributes a large fraction of the selected $B^\pm \to D(\to K^0_S\pi^+\pi^-)K^\pm$ candidates. Partially reconstructed candidates from decay modes containing a $D \to K^0_S\pi^+\pi^-$ decay, such as $B^\pm \to D^*h^\pm$ (where D^* represents D^{*0} or $\overline{D}^{*0}$ and $h^\pm$ represents a $K^\pm$ or $\pi^\pm$), $B_{(s)} \to DK^*$ (where $B_{(s)}$ represents $B^0_{(s)}$ or $\overline{B}^0_{(s)}$ and K^* represents K^{*0} or $\overline{K}^{*0}$) and $B^\pm \to D\rho^\pm$ decays, are also expected to contribute. The contributions from charmless $B^\pm$ decays, $B^\pm \to D(\to K^0_S K^\pm\pi^\mp)h^\pm$ decays, $B^\pm \to D(\to K^0_S K^+K^-)h^\pm$ decays and $B^\pm \to D(\to \pi^+\pi^-h^+h^-)h^\pm$ decays are found to be negligible.

4. Analysis strategy

The analysis is performed in two distinct parts. The fractions of signal and background are determined with a phase-space integrated fit to the invariant mass distributions, m_{Dh}, of selected $B^\pm \to D(\to K^0_S\pi^+\pi^-)K^\pm$ and $B^\pm \to D(\to K^0_S\pi^+\pi^-)\pi^\pm$ candidates, shown in Fig. 1. This is followed by a fit to determine the CP violation observables $(x_\pm, y_\pm)$ and the variation in efficiency over the phase space of the $D \to K^0_S\pi^+\pi^-$ decay. The relative signal and background yields and the parameters of the $B^\pm$ invariant mass probability distribution functions (PDFs) are fixed to the values determined in the first stage.

4.1. Invariant mass fit of $B^\pm$ candidates

An unbinned extended maximum likelihood fit to the invariant mass distributions of the $B^\pm$ candidates determines the signal and background fractions. The samples of $B^\pm \to D(\to K^0_S\pi^+\pi^-)K^\pm$ and $B^\pm \to D(\to K^0_S\pi^+\pi^-)\pi^\pm$ candidates are fitted simultaneously in an invariant mass range of $4779\ \text{MeV}/c^2 < m_{Dh} < 5779\ \text{MeV}/c^2$. The *long* and *downstream* candidates are fitted separately.

For the fit to the $B^\pm \to D(\to K^0_S\pi^+\pi^-)K^\pm$ invariant mass distribution, the total PDF is composed of a signal and several background components. The signal ($B^\pm \to DK^\pm$) is described by

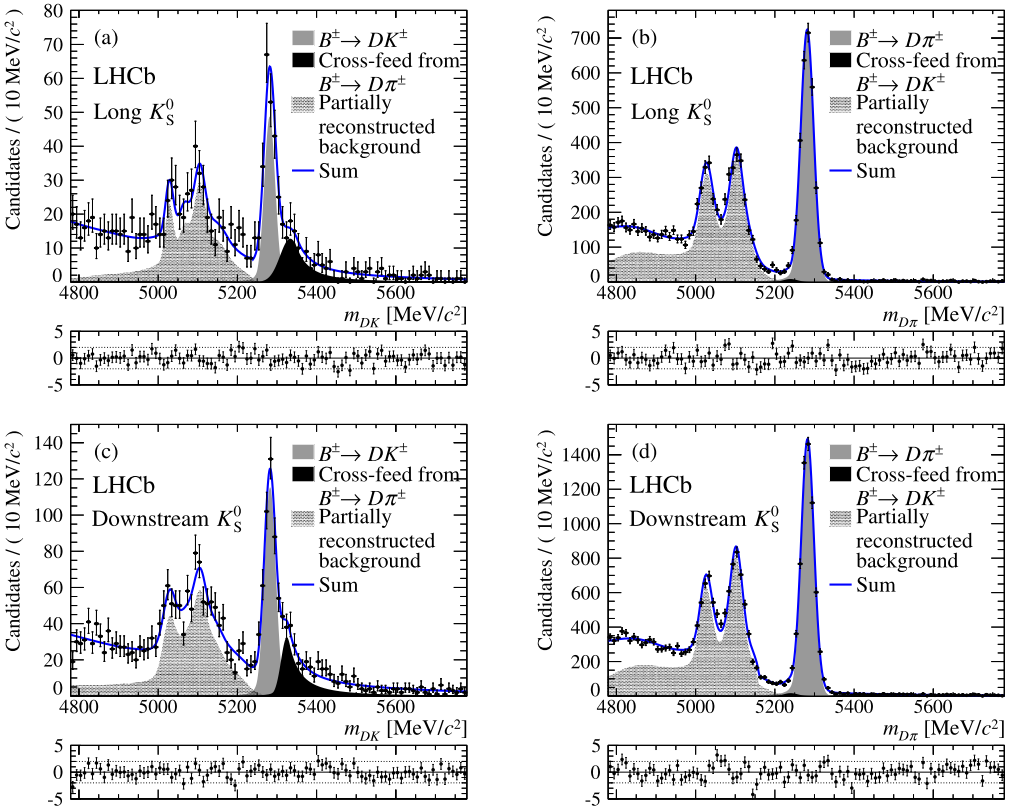

Fig. 1. Invariant mass distributions for (a) $B^\pm \to D(\to K^0_S\pi^+\pi^-)K^\pm$ *long*, (b) $B^\pm \to D(\to K^0_S\pi^+\pi^-)\pi^\pm$ *long*, (c) $B^\pm \to D(\to K^0_S\pi^+\pi^-)K^\pm$ *downstream* and (d) $B^\pm \to D(\to K^0_S\pi^+\pi^-)\pi^\pm$ *downstream* candidates. The fit results, including signal and background components, are superimposed. The lower plots are normalised residual distributions.

the sum of a Crystal Ball [24] and a Gaussian function with common means. The Crystal Ball tail parameters, the width of the Gaussian function and the relative fractions of both functions are fixed to values obtained from simulated data. An exponential function describes the two categories of combinatorial background candidates. Cross-feed candidates are characterised by a Crystal Ball function with tails on both upper and lower sides. The mean and tail parameters of the function are fixed to results from simulation. Partially reconstructed background contributions are described by various functions with parameters fixed to values obtained from simulation. Both B and $B^\pm$ decays that give rise to candidates with similar invariant mass distributions are described by a single fit component: the candidates from $B^\pm \to D^*K^\pm$ and $B \to D^{*\mp}K^\pm$ decays are both described using the sum of two pairs of Gaussian functions, where the Gaussian functions in each pair have a common mean and independent widths. For the combined background contribution from partially reconstructed $B^\pm \to D^*\pi^\pm$ and $B \to D^{*\mp}\pi^\pm$ decays, labelled $D^*\pi$, the sum of two Crystal Ball functions, each with tails on both upper and lower sides, is used. A background composed of candidates from $B \to D\rho^0$ and $B^\pm \to D\rho^\pm$ decays, labelled $D\rho$, is described by the sum of a Gaussian and an exponential function. A Gaussian function is included for background candidates partially reconstructed from $B \to D^{*\mp}\rho^\pm$ and

$B^\pm \to D^*\rho^\pm$ decays. The background contribution from partially reconstructed $B \to DK^*$ decays is modelled by the convolution of an ARGUS function [25] with a Gaussian function; the same convolution of functions is used for candidates reconstructed from $B_s \to DK^*$ decays.

For the fit to the $B^\pm \to D(\to K^0_S\pi^+\pi^-)\pi^\pm$ mass distribution, the same PDFs are used for signal, combinatorial and cross-feed background contributions as for the fit to the $B^\pm \to D(\to K^0_S\pi^+\pi^-)K^\pm$ distribution. The analogous function parameters are fixed to the results of fits to simulation. Again, functions are also included for partially reconstructed background candidates, with all parameters fixed to values obtained from simulation. The sum of two pairs of Gaussian functions, labelled $D^*\pi$, is used for the background from partially reconstructed $B^\pm \to D^*\pi^\pm$ and $B \to D^{*\mp}\pi^\pm$ decays. Partially reconstructed $B \to D\rho^0$ and $B^\pm \to D\rho^\pm$ decays are described by the convolution of an ARGUS function with a Gaussian function. A Gaussian function is used to describe background from partially reconstructed $B \to D^{*\mp}\rho^\pm$ and $B^\pm \to D^*\rho^\pm$ decays.

In the simultaneous fit, the mean values of the signal functions in $B^\pm \to DK^\pm$ and $B^\pm \to D\pi^\pm$ are constrained to a common value.

The yield of the cross-feed component in the fit to the $B^\pm \to DK^\pm$ ($B^\pm \to D\pi^\pm$) distribution is fixed with respect to the signal yield in the $B^\pm \to D\pi^\pm$ ($B^\pm \to DK^\pm$) distribution, using knowledge of the efficiency and misidentification rate of the PID criterion separating the $B^\pm \to DK^\pm$ and $B^\pm \to D\pi^\pm$ candidate samples. Large calibration samples of kaons and pions from $D^{*\pm} \to D(\to K^\mp\pi^\pm)\pi^\pm$ decays, kinematically selected from data, are reweighted to match the kinematic properties of the bachelor tracks in the $B^\pm \to D\pi^\pm$ *long* and *downstream* candidate samples and are then used to determine the relevant efficiencies. The remaining background yields are free to vary in the fit, as are the remaining PDF parameters and the ratio of the signal yields.

Since it is not possible to separate the two components of combinatorial background with the fit to the $B^\pm$ invariant mass distributions, the yield of combinatorial D background candidates is estimated from data using $B^\pm \to Dh^\pm$ decays, where the D is reconstructed to decay to two same-sign pions ($D \to K^0_S\pi^+\pi^+$ and charge conjugate). These "wrong-sign" decays are subject to the selection criteria described in Section 3.

4.2. *CP asymmetry fit*

The distributions in the $D \to K^0_S\pi^+\pi^-$ decay phase space for positively and negatively charged $B^\pm \to D(\to K^0_S\pi^+\pi^-)K^\pm$ and $B^\pm \to D(\to K^0_S\pi^+\pi^-)\pi^\pm$ candidate decays are fitted simultaneously using an unbinned maximum likelihood fit to determine the *CP* violation observables $(x_\pm, y_\pm)$ and the variation in efficiency over the phase space. Although $B^\pm \to D(\to K^0_S\pi^+\pi^-)\pi^\pm$ decays are expected to exhibit interference analogous to $B^\pm \to D(\to K^0_S\pi^+\pi^-)K^\pm$ decays and therefore be sensitive to γ, the magnitude of the ratio of interfering D decay amplitudes, $r_{B^\pm \to D\pi^\pm}$, is expected to be an order of magnitude smaller than r_B for $B^\pm \to D(\to K^0_S\pi^+\pi^-)K^\pm$ decays. It is therefore possible, to a good approximation, to neglect the suppressed contribution to the $B^\pm \to D(\to K^0_S\pi^+\pi^-)\pi^\pm$ decay amplitude and use $B^\pm \to D(\to K^0_S\pi^+\pi^-)\pi^\pm$ decays to obtain the efficiency variation as a function of m^2_+ and m^2_-, which is modelled as a second-order polynomial function. This assumption is considered as a source of systematic uncertainty.

The candidates are divided into eight subsamples, according to K^0_S type (*long* or *downstream*), the charge of the bachelor track, and whether the candidate is identified as a $B^\pm \to DK^\pm$ or $B^\pm \to D\pi^\pm$ decay. The negative logarithm of the likelihood,

$$-\ln\mathcal{L} = -\sum_s \sum_k \ln\left(\sum_c N_c \cdot p_{cs}^{\text{mass}}\left((m_{Dh})_k; \vec{P}_{cs}^{\text{mass}}\right) \cdot p_{cs}^{\text{model}}\left(\left(m_+^2, m_-^2\right)_k; \vec{P}_{cs}^{\text{model}}\right)\right), \tag{2}$$

is minimised; in this expression, c indexes the candidate categories (signal or background type), s indexes the subsample, and k identifies each decay candidate. N_c is the candidate yield for category c, and p_{cs}^{mass} is the invariant mass PDF, p_{cs}^{model} is the normalised D decay model described below, $\vec{P}_{cs}^{\text{mass}}$ are the mass PDF parameters, and $\vec{P}_{cs}^{\text{model}}$ are the D decay model parameters for category c and subsample s. It should be noted that $(x_\pm, y_\pm)$ are included in the parameter list of the $B^\pm \to DK^\pm$ signal category and the $B^\pm \to D\pi^\pm$ cross-feed category, which arises from misidentification of $B^\pm \to DK^\pm$ decays. The normalisation of p_{cs}^{model} depends on the efficiency variation over the phase space. The yields and parameters of the mass PDFs are fixed to the results obtained in the $B^\pm$ invariant mass fit. To avoid inadvertent experimenter's bias in the determination of the *CP* violation parameters, the values of the observables $(x_\pm, y_\pm)$ are masked until the measurement technique has been finalised.

The model describing the amplitude of the $D \to K^0_S\pi^+\pi^-$ decay over the phase space, $A_f(m_+^2, m_-^2)$, is identical to that used by the BaBar Collaboration in Refs. [5,26]. It incorporates an isobar model for P-wave (which includes $\rho(770)$, $\omega(782)$, Cabibbo-allowed and doubly Cabibbo-suppressed $K^*(892)$ and $K^*(1680)$) and D-wave (including $f_2(1270)$ and $K_2^*(1430)$) contributions. A generalised LASS amplitude for the $K\pi$ S-wave contribution ($K_0^*(1430)$) and a K-matrix with P-vector approach for the $\pi\pi$ S-wave contribution are also included in the model. All parameters of the model are fixed in the fit to the values determined in Ref. [26].[1]

The fit is performed using refitted candidates with a $B^\pm$ invariant mass lying within $\pm 50\,\text{MeV}/c^2$ around the known value [22], corresponding to an invariant mass region of approximately $\pm 3\sigma$ around the signal peak. Although the full description of the mass PDF provides valuable constraints for the background within the mass window, only those backgrounds with significant contributions are included in the *CP* asymmetry fit. The yields of the signal and incorporated background contributions are given in Table 1. For the $B^\pm \to DK^\pm$ subsamples, the cross-feed, combinatorial D, random Dh, $D^*\pi$, $D\rho$ and $B_s \to DK^*$ background categories are included in the fit. The cross-feed contribution is assumed to be distributed in the phase space of the $D \to K^0_S\pi^+\pi^-$ decay according to the $D^0 \to K^0_S\pi^+\pi^-$ ($\overline{D}^0 \to K^0_S\pi^+\pi^-$) decay model in the $B^- \to DK^-$ ($B^+ \to DK^+$) case. Combinatorial D background candidates are expected to be distributed non-resonantly over the phase space. The distribution of random Dh candidates is assumed to be an incoherent sum of the $D^0 \to K^0_S\pi^+\pi^-$ and $\overline{D}^0 \to K^0_S\pi^+\pi^-$ decay models. Both $B^\pm \to D^*\pi^\pm$ and $B \to D^{*\mp}\pi^\pm$ decays are represented by the inclusion of a $D^0 \to K^0_S\pi^+\pi^-$ ($\overline{D}^0 \to K^0_S\pi^+\pi^-$) decay model in the $B^- \to DK^-$ ($B^+ \to DK^+$) case. The $D\rho$ component of the invariant mass fit is composed of candidates from $B \to D\rho^0$ and $B^\pm \to D\rho^\pm$ decays; the distribution of candidates from $B \to D\rho^0$ over the $D \to K^0_S\pi^+\pi^-$ decay phase space is assumed to be an incoherent sum of the $D^0 \to K^0_S\pi^+\pi^-$ and $\overline{D}^0 \to K^0_S\pi^+\pi^-$ decay models, whereas the candidates from $B^\pm \to D\rho^\pm$ are accounted for with a $D^0 \to K^0_S\pi^+\pi^-$ ($\overline{D}^0 \to K^0_S\pi^+\pi^-$) decay model for the $B^- \to DK^-$ ($B^+ \to DK^+$) case. Background $B_s \to DK^*$ candidates are

[1] The model implemented by BaBar [26] differs from the formulation described therein. One of the two Blatt–Weisskopf coefficients was set to unity, and the imaginary part of the denominator of the Gounaris–Sakurai propagator used the mass of the resonant pair, instead of the mass associated with the resonance. The model used herein replicates these features without modification. It has been verified that changing the model to use an additional centrifugal barrier term and a modified Gounaris–Sakurai propagator has a negligible effect on the measurements.

Table 1
Signal and background yields for components contributing to the *CP* asymmetry fit, in the region ± 50 MeV/c^2 around the known $B^\pm$ meson mass.

Fit component	$B^\pm \to DK^\pm$, *long*	$B^\pm \to DK^\pm$, *downstream*
Signal	217 ± 17	420 ± 27
Backgrounds		
Cross-feed (from $B^\pm \to D\pi^\pm$)	35.9 ± 0.7	76 ± 1
Combinatorial D	5^{+7}_{-3}	31^{+11}_{-9}
Random Dh	28^{+5}_{-8}	45^{+18}_{-19}
$D^*\pi$	0.36 ± 0.08	6 ± 7
$D\rho$	2.2 ± 0.5	4 ± 11
$B_s \to DK^*$	0.9 ± 0.2	4 ± 2
Fit component	$B^\pm \to D\pi^\pm$, *long*	$B^\pm \to D\pi^\pm$, *downstream*
Signal	2906 ± 56	5960 ± 80
Backgrounds		
Cross-feed (from $B^\pm \to DK^\pm$)	27 ± 2	53 ± 3
Combinatorial D	15^{+19}_{-10}	99^{+36}_{-27}
Random Dh	76^{+15}_{-22}	146^{+33}_{-41}
$D^*\pi$	6.6 ± 0.4	22.0 ± 0.7

assumed to be distributed according to the $\overline{D}^0 \to K^0_S\pi^+\pi^-$ ($D^0 \to K^0_S\pi^+\pi^-$) decay model in the $B^- \to DK^-$ ($B^+ \to DK^+$) case. For the $B^\pm \to D\pi^\pm$ subsamples, contributions from cross-feed, combinatorial D, random Dh, and $D^*\pi$ background types are included in the fit. The cross-feed candidates in $B^\pm \to D\pi^\pm$ arise from misidentification of the bachelor track of $B^\pm \to DK^\pm$ decays; the candidates are assumed to be distributed accordingly. The remaining combinatorial and $D^*\pi$ background contributions are assumed to be distributed as described above.

Figs. 2–5 show the $B^\pm \to D(\to K^0_S\pi^+\pi^-)\pi^\pm$ and $B^\pm \to D(\to K^0_S\pi^+\pi^-)K^\pm$ candidate Dalitz plot distributions and their projections, with the results of the fit superimposed. The resulting measured values of $(x_\pm, y_\pm)$ are

$$x_- = +0.027 \pm 0.044,$$
$$y_- = +0.013 \pm 0.048,$$
$$x_+ = -0.084 \pm 0.045,$$
$$y_+ = -0.032 \pm 0.048,$$

where the uncertainties are statistical only. The corresponding likelihood contours are shown in Fig. 6.

5. Systematic uncertainties

Systematic uncertainties on the measured values of $(x_\pm, y_\pm)$ arising from various sources are considered and summarised in Table 2. Unless otherwise stated, for each source considered the *CP* asymmetry fit is repeated with the efficiency parameters and $(x_\pm, y_\pm)$ allowed to vary, as in the nominal fit to data. The resulting differences in the values of $(x_\pm, y_\pm)$ from the nominal results are taken as systematic uncertainties.

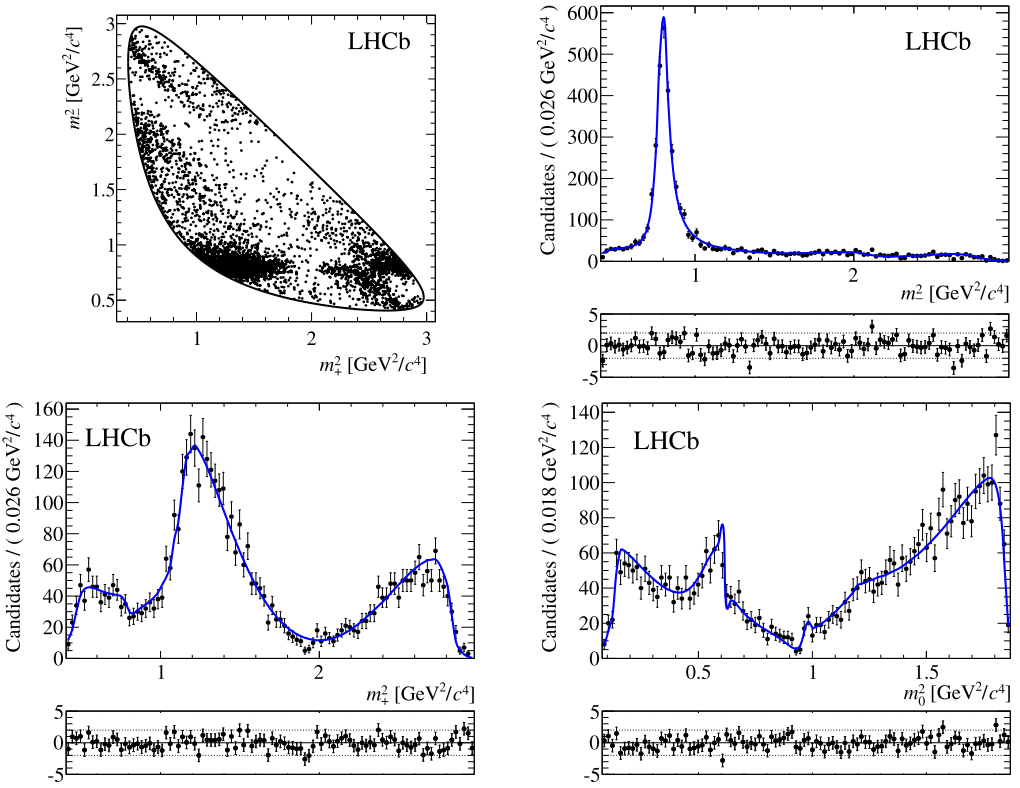

Fig. 2. Dalitz plot and its projections, with fit result superimposed, for $B^- \to D\pi^-$ candidates; $m^2_\pm \equiv m^2_{K^0_S\pi^\pm}$ and $m^2_0 \equiv m^2_{\pi^+\pi^-}$. The lower parts of the figures are normalised residual distributions.

The fractions of signal and background are estimated with a fit to the $B^\pm$ candidate invariant mass distributions. To find the systematic uncertainties in $(x_\pm, y_\pm)$ arising from the uncertainties in these fractions, the shapes and yields of the individual mass PDF contributions are modified and the fit repeated. The largest changes in $(x_\pm, y_\pm)$ arise from modifications to the cross-feed and total combinatorial background components. The uncertainties are therefore evaluated by repeating the *CP* asymmetry fit with the cross-feed and total combinatorial background yields independently varied by their statistical uncertainties.

The yield of combinatorial D background is estimated using wrong-sign candidates selected from data. The systematic uncertainties arising from these estimates are found by repeating the *CP* asymmetry fit to data with the yields varied by the statistical uncertainties shown in Table 1. Corresponding variations in the random Dh background yield are made, so that the total combinatorial background yield, obtained from the $B^\pm$ invariant mass fit, is unchanged.

In the $B^\pm$ invariant mass fit, a component PDF for partially reconstructed $B^\pm \to D(\to K^0_S\pi^+\pi^-)\mu^\pm\nu$ background is not included. The systematic uncertainty arising from this omission is found by repeating the *CP* asymmetry fit to data with a contribution from this background. The upper limits on the yields and the mass functions are found by applying muon identification requirements to the bachelor tracks of data candidates, and are kept constant in the fit.

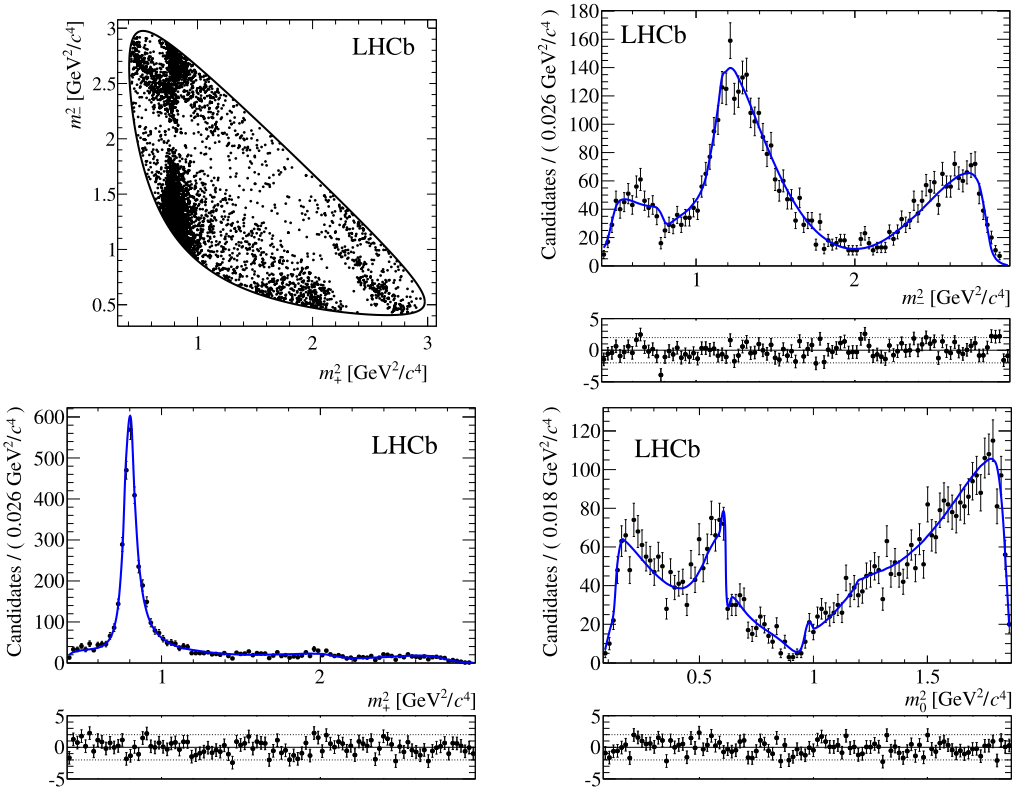

Fig. 3. Dalitz plot and its projections, with fit result superimposed, for $B^+ \to D\pi^+$ candidates; $m^2_\pm \equiv m^2_{K^0_S\pi^\pm}$ and $m^2_0 \equiv m^2_{\pi^+\pi^-}$. The lower parts of the figures are normalised residual distributions.

In the *CP* asymmetry fit, the background fractions obtained from the invariant mass fit to $B^\pm$ candidates are used for both B^+ and B^- candidates. This neglects any detection asymmetries for the charged bachelor tracks. The *CP* asymmetry fit is repeated with the central value of the charged kaon asymmetry, $(-1.2 \pm 0.2)\%$ [27], introduced for the signal and background components where the bachelor is expected to be a kaon.

In the *CP* asymmetry fit, combinatorial D background candidates are assumed to be distributed non-resonantly over the phase space of the $D \to K^0_S\pi^+\pi^-$ decay. The *CP* asymmetry fit is repeated with the D decay model changed to the sum of a phase-space distribution and a $K^{*\pm}(892)$ resonance; the fractions of the two components are fixed by a study of the Dalitz plot projections of data.

The D decay model included in the *CP* asymmetry fit for random Dh background candidates is an incoherent sum of the two $D \to K^0_S\pi^+\pi^-$ decay amplitudes because it is equally likely for a D^0 or $\overline{D}^0$ meson to be present in an event. The *CP* asymmetry fit is repeated with the decay model changed to include the central value of the $D^0 - \overline{D}^0$ production asymmetry of $(-1.0 \pm 0.3)\%$ [28].

The yield of $B_s \to DK^*$ partially reconstructed background candidates is very low in the signal invariant mass region, but in the *CP* asymmetry fit the candidates are assumed to be distributed in the same way as the suppressed component of signal $B^\pm \to DK^\pm$ over the

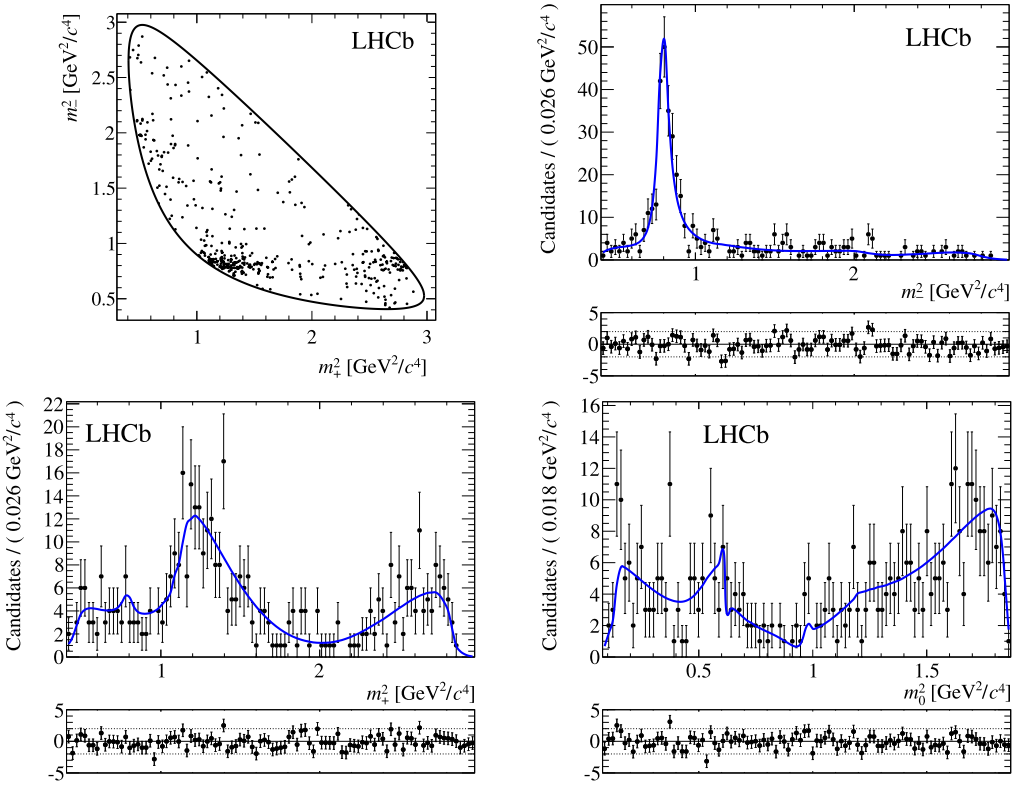

Fig. 4. Dalitz plot and its projections, with fit result superimposed, for $B^- \to DK^-$ candidates; $m^2_\pm \equiv m^2_{K^0_S\pi^\pm}$ and $m^2_0 \equiv m^2_{\pi^+\pi^-}$. The lower parts of the figures are normalised residual distributions.

$D \to K^0_S\pi^+\pi^-$ decay phase space and could therefore appear in particularly sensitive regions. To estimate the systematic uncertainty arising from the assumed distribution, the *CP* asymmetry fit to data is performed with the D decay model for this background changed to the favoured component of the signal $B^\pm \to DK^\pm$ decay model.

In order to allow the candidate detection, reconstruction and selection efficiency variation across the phase space of the $D \to K^0_S\pi^+\pi^-$ decay to be found from $B^\pm \to D\pi^\pm$ data candidates, the amplitudes from the suppressed decays $B^- \to \overline{D}{}^0\pi^-$ and $B^+ \to D^0\pi^+$ are assumed to be negligible. The systematic uncertainty arising from this assumption is estimated by repeating the *CP* asymmetry fit to data with an additional term in the signal $B^\pm \to D\pi^\pm$ and cross-feed $B^\pm \to DK^\pm$ decay models, representing the suppressed decay amplitudes. The values of $r_{B^\pm\to D\pi^\pm}$, $\delta_{B^\pm\to D\pi^\pm}$ and γ are fixed in the additional term; various $r_{B^\pm\to D\pi^\pm}$ and $\delta_{B^\pm\to D\pi^\pm}$ values are assumed ($r_{B^\pm\to D\pi^\pm} = 0.01, 0.015$; $\delta_{B^\pm\to D\pi^\pm} = 0°, 90°, 180°, 270°, 315°$), but in all cases γ is set to 70°.

The efficiency variation across the $D \to K^0_S\pi^+\pi^-$ decay phase space is parametrised in the *CP* asymmetry fit by a second-order polynomial function in the variables m^2_+ and m^2_-. To estimate the uncertainty arising from this, the *CP* asymmetry fit to data is repeated with the efficiency parametrisation fixed and variations of the polynomial coefficients made. A fit with a third-order polynomial function is also performed, with the efficiency parameters and $(x_\pm, y_\pm)$ allowed to

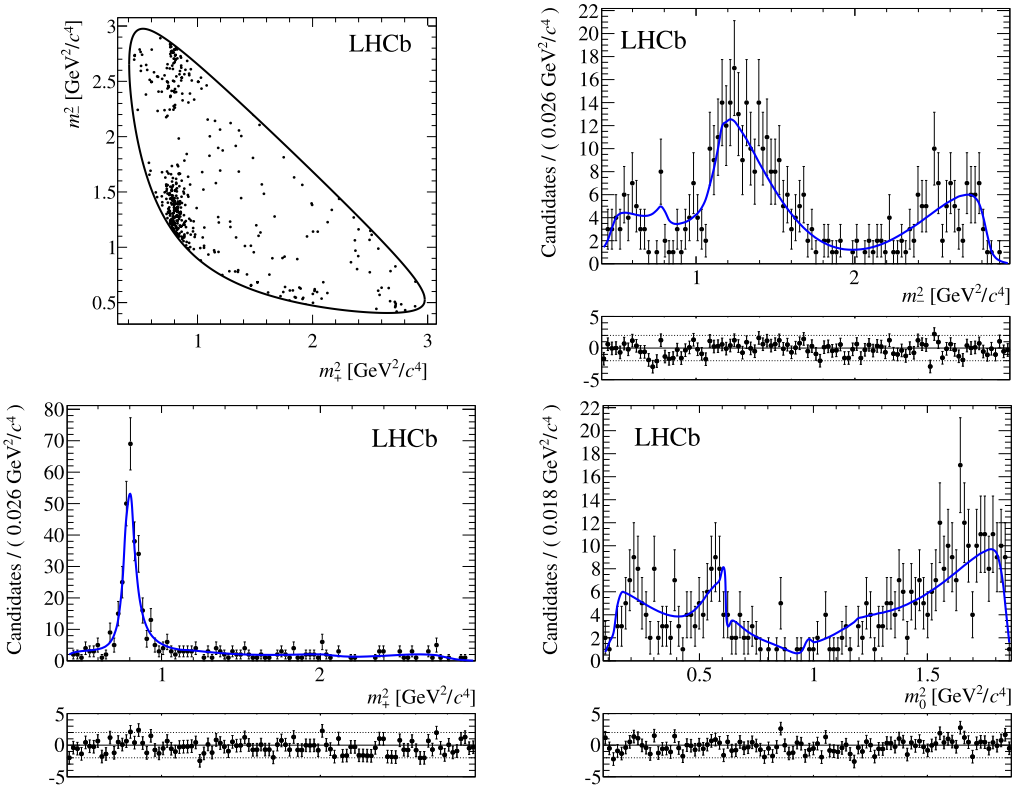

Fig. 5. Dalitz plot and its projections, with fit result superimposed, for $B^+ \to DK^+$ candidates; $m^2_\pm \equiv m^2_{K^0_S\pi^\pm}$ and $m^2_0 \equiv m^2_{\pi^+\pi^-}$. The lower parts of the figures are normalised residual distributions.

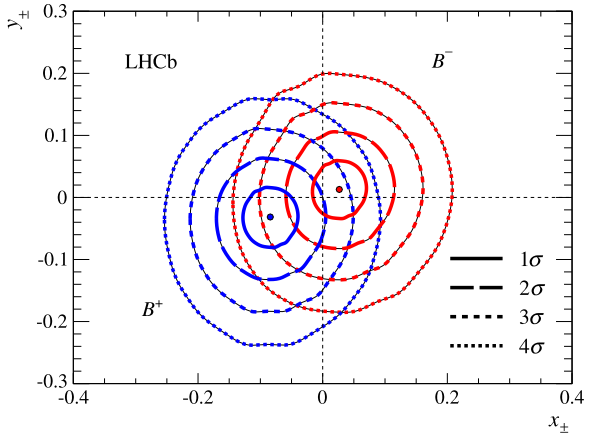

Fig. 6. Likelihood contours at 39.35%, 86.47%, 98.89% and 99.97% confidence level for (x_+, y_+) (blue in the web version) and (x_-, y_-) (red in the web version).

Table 2
Absolute values of systematic uncertainties. The *CP* asymmetry fit bias is considered as a one-sided uncertainty and is included in the quadrature sum on that side only.

Source	$\delta x_-(\times 10^{-3})$	$\delta y_-(\times 10^{-3})$	$\delta x_+(\times 10^{-3})$	$\delta y_+(\times 10^{-3})$
Background yields				
Cross-feed	0.21	0.96	0.65	0.26
Total combinatorial	1.1	3.5	1.7	2.7
Combinatorial D	1.0	4.3	2.7	4.9
Inclusion of semileptonic background	3.1	2.8	0.63	3.2
Charged kaon detection asymmetry	0.022	0.030	0.0041	0.025
Amplitudes for backgrounds				
Combinatorial D	3.5	3.4	4.7	6.4
Random Dh	0.10	0.16	0.066	0.16
B_s partially reconstructed	0.59	0.59	0.15	0.73
$r_{B^\pm \to D\pi^\pm}$	1.8	1.9	1.6	1.1
Efficiency over the phase space	5.7	0.35	6.9	0.31
CP asymmetry fit bias	$^{+5.7}_{-0}$	$^{+5.1}_{-0}$	$^{+0}_{-1.3}$	$^{+2.6}_{-0}$
Total experiment or fit related	$^{+9.6}_{-7.8}$	$^{+9.0}_{-7.4}$	$^{+9.1}_{-9.2}$	$^{+9.6}_{-9.2}$
Total model related	1.0	3.0	4.6	8.4

Table 3
Model related systematic uncertainties for each alternative model. The relative signs indicate full correlation or anti-correlation.

	Description		$\delta x_-(\times 10^{-3})$	$\delta y_-(\times 10^{-3})$	$\delta x_+(\times 10^{-3})$	$\delta y_+(\times 10^{-3})$
(a)	K-matrix 1st solution		−0.1	0.04	0.3	−2
(b)	K-matrix 2nd solution		−0.09	−0.3	0.1	−0.5
(c)	Remove slowly varying part in P-vector		−0.1	−0.3	0.1	−0.8
(d)	Generalised LASS → relativistic Breit–Wigner		−0.7	−2	3	7
(e)	Gounaris–Sakurai → relativistic Breit–Wigner		0.08	−0.8	0.1	0.8
(f)	$K^*(1680)$	$m + \delta m$	−0.06	−0.6	0.2	0.3
(g)		$m - \delta m$	−0.1	−0.2	−0.1	−1
(h)		$\Gamma + \delta\Gamma$	−0.06	−0.4	−0.05	−0.4
(i)		$\Gamma - \delta\Gamma$	−0.2	−0.3	0.3	−0.5
(j)	$f_2(1270)$	$m + \delta m$	−0.1	−0.3	0.1	−0.5
(k)		$m - \delta m$	−0.1	−0.4	0.09	−0.5
(l)		$\Gamma + \delta\Gamma$	−0.1	−0.3	0.08	−0.5
(m)		$\Gamma - \delta\Gamma$	−0.1	−0.4	0.1	−0.5
(n)	$K_2^*(1430)$	$m + \delta m$	−0.08	−0.4	0.08	−0.4
(o)		$m - \delta m$	−0.1	−0.3	0.1	−0.5
(p)		$\Gamma + \delta\Gamma$	−0.1	−0.4	0.07	−0.4
(q)		$\Gamma - \delta\Gamma$	−0.1	−0.3	0.1	−0.5
(r)	$r_{\rm BW} = 0.0\ {\rm GeV}^{-1}$		−0.2	−0.4	−0.1	−0.3
(s)	$r_{\rm BW} = 3.0\ {\rm GeV}^{-1}$		−0.3	−0.3	1	−0.4
(t)	Add $K^*(1410)$ and $\rho(1450)$		−0.1	−0.3	0.02	−0.7
(u)	Helicity formalism		−0.5	−2	−3	4

vary. The changes in the values of $(x_\pm, y_\pm)$, compared to the nominal results, are taken as the systematic uncertainties arising from the efficiency parametrisation.

The *CP* asymmetry fit is verified using 1000 data-sized simulated pseudo-experiments. In each experiment the number and distribution of candidates is generated according to the fit result from data. The obtained values of $(x_\pm, y_\pm)$ show a small bias when compared to the values used for the simulation; these biases are included as systematic uncertainties.

To estimate the systematic uncertainty arising from the choice of amplitude model description of the $D \to K^0_S\pi^+\pi^-$ decay, *CP* asymmetry fits with alternative model descriptions are performed on large samples of simulated decays. For each alternative model, one element (for example, a resonance parameter) of the nominal model is altered. One million $B^\pm \to D\pi^\pm$ and one million $B^\pm \to DK^\pm$ decays are simulated with the model used for the nominal *CP* asymmetry fit, and with the Cartesian parameters fixed to the fit result. For the nominal model and each alternative model, a *CP* asymmetry fit to the $B^\pm \to D\pi^\pm$ sample is performed with the coefficients of each resonance of the model allowed to vary. Values for the Cartesian parameters $(x_\pm, y_\pm)$ are then obtained from a *CP* asymmetry fit to the $B^\pm \to DK^\pm$ sample, with the resonance coefficients fixed from the results of the fit to the $B^\pm \to D\pi^\pm$ sample. The signed differences in the values of $(x_\pm, y_\pm)$ from the nominal results are taken as the systematic uncertainties, with the relative signs between contributions indicating full correlation or anti-correlation.

In the alternative models considered, the following changes, labelled (a)–(u), have been applied, resulting in the uncertainties summarised in Table 3:

- $\pi\pi$ S-wave: The F-vector model is changed to use two other solutions of the K-matrix (from a total of three) determined from fits to scattering data [29] (a), (b). The slowly varying part of the non-resonant term of the P-vector is removed (c).
- $K\pi$ S-wave: The generalised LASS parametrisation, used to describe the $K^*_0(1430)$ resonance, is replaced by a relativistic Breit–Wigner propagator with parameters taken from Ref. [30] (d).
- $\pi\pi$ P-wave: The Gounaris–Sakurai propagator is replaced by a relativistic Breit–Wigner propagator (e).
- $K\pi$ P-wave: The mass and width of the $K^*(1680)$ resonance are varied by their uncertainties from Ref. [31] (f)–(i).
- $\pi\pi$ D-wave: The mass and width of the $f_2(1270)$ resonance are varied by their uncertainties from Ref. [22] (j)–(m).
- $K\pi$ D-wave: The mass and width of the $K^*_2(1430)$ resonance are varied by their uncertainties from Ref. [22] (n)–(q).
- The radius of the Blatt–Weisskopf centrifugal barrier factors, $r_{\rm BW}$, is changed from 1.5 GeV^{-1} to 0.0 GeV^{-1} (r) and 3.0 GeV^{-1} (s).
- Two further resonances, $K^*(1410)$ and $\rho(1450)$, parametrised with relativistic Breit–Wigner propagators, are included in the model (t).
- The Zemach formalism used for the angular distribution of the decay products is replaced by the helicity formalism (u).

The total covariance matrix is determined to be

$$V_{\text{model}} = \begin{array}{c} \begin{matrix} x_- & y_- & x_+ & y_+ \end{matrix} \\ \begin{pmatrix} 1.12 & 2.80 & -0.95 & -5.40 \\ 2.80 & 8.89 & -1.21 & -16.87 \\ -0.95 & -1.21 & 21.59 & 5.97 \\ -5.40 & -16.87 & 5.97 & 69.87 \end{pmatrix} \end{array} \times 10^{-6} \tag{3}$$

resulting in total systematic uncertainties arising from the choice of amplitude model of

$$\begin{aligned} \delta x_- &= 1.0 \times 10^{-3}, \\ \delta y_- &= 3.0 \times 10^{-3}, \\ \delta x_+ &= 4.6 \times 10^{-3}, \\ \delta y_+ &= 8.4 \times 10^{-3}. \end{aligned}$$

Table 2 summarises the systematic uncertainties arising from all sources. Except for the uncertainty due to the fit bias, the absolute values of the uncertainties are added in quadrature (assuming no correlation) to obtain the total experiment or fit related uncertainties. The *CP* asymmetry fit bias is considered as a one-sided uncertainty and is included in the quadrature sum on that side only. The model related systematic uncertainty is also shown in the table, for comparison.

6. Constraints on γ, r_B and δ_B

The results for the *CP* violation observables $(x_\pm, y_\pm)$ are used to place constraints on the values of γ, r_B and δ_B, adopting the procedure described in Refs. [9,10].

There is a two-fold ambiguity in the solution for γ, r_B and δ_B; choosing the solution that satisfies $(0 < \gamma < 180)^\circ$ leads to the results

$$\begin{aligned} \gamma &= \left(84^{+49}_{-42}\right)^\circ, \\ r_B &= 0.06 \pm 0.04, \\ \delta_B &= \left(115^{+41}_{-51}\right)^\circ, \end{aligned}$$

where the uncertainties include statistical, experimental systematic and model related systematic contributions. Fig. 7 shows the contours of p-value projected onto the (γ, δ_B) and (γ, r_B) planes.

7. Effect of neutral D meson mixing

Assuming uniform lifetime acceptance, the measurements of the Cartesian parameters documented in this paper are corrected for the effects of D mixing as described in Ref. [32],

$$\begin{aligned} x_\pm^{\text{corr}} &= x_\pm + \frac{y_{\text{mix}}}{2}, \\ y_\pm^{\text{corr}} &= y_\pm + \frac{x_{\text{mix}}}{2}, \end{aligned}$$

where x_{mix} and y_{mix} are the parameters of neutral D meson mixing.

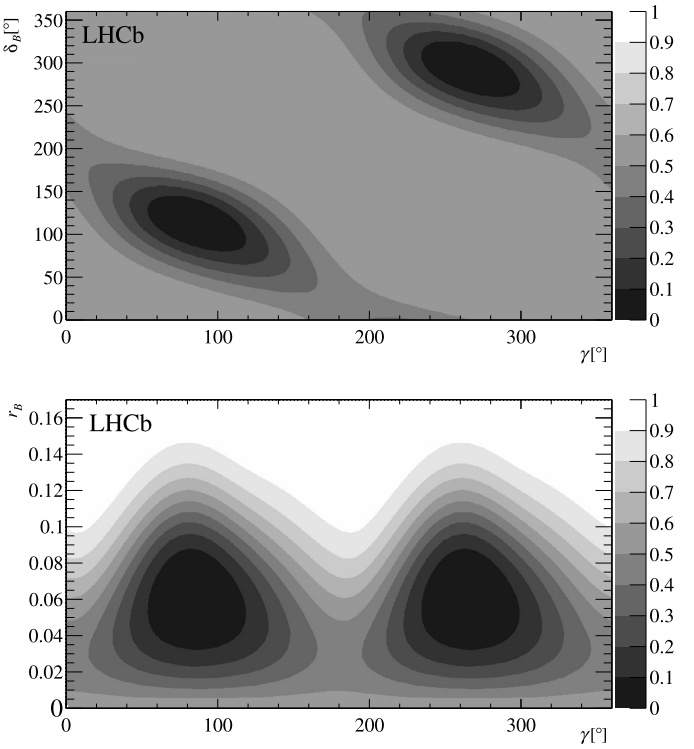

Fig. 7. Projections of the p-value regions onto the (γ, δ_B) and (γ, r_B) planes with all sources of uncertainty taken into account.

Since *CP* violation in the charm sector has been neglected in the analysis, the world average values of the mixing parameters without *CP* violation ($x_{\rm mix} = (0.53^{+0.16}_{-0.17}) \times 10^{-2}$, $y_{\rm mix} = (0.67 \pm 0.09) \times 10^{-2}$) [33] are taken for correction, yielding the values

$$x_-^{\rm corr} = +0.030 \pm 0.044^{+0.010}_{-0.008} \pm 0.001 \pm 0.00045,$$
$$y_-^{\rm corr} = +0.016 \pm 0.048^{+0.009}_{-0.007} \pm 0.003 \pm 0.00085,$$
$$x_+^{\rm corr} = -0.081 \pm 0.045 \pm 0.009 \pm 0.005 \pm 0.00045,$$
$$y_+^{\rm corr} = -0.029 \pm 0.048^{+0.010}_{-0.009} \pm 0.008 \pm 0.00085,$$

where the first uncertainty is statistical, the second systematic, the third arises from the D decay amplitude model and the fourth is the uncertainty associated with the values of the mixing parameters. The change in the value of γ due to this correction is less than 1°.

8. Conclusions

Candidate $B^\pm \to D(\to K^0_S\pi^+\pi^-)K^\pm$ decays are used to perform an amplitude analysis incorporating a model description of the $D \to K^0_S\pi^+\pi^-$ decay. The data used correspond to an integrated luminosity of 1 fb^{-1}, recorded by LHCb at a centre-of-mass energy of 7 TeV in 2011.

The resulting values of the *CP* violation observables $x_\pm = r_B \cos(\delta_B \pm \gamma)$ and $y_\pm = r_B \sin(\delta_B \pm \gamma)$ are

$$x_- = +0.027 \pm 0.044^{+0.010}_{-0.008} \pm 0.001,$$
$$y_- = +0.013 \pm 0.048^{+0.009}_{-0.007} \pm 0.003,$$
$$x_+ = -0.084 \pm 0.045 \pm 0.009 \pm 0.005,$$
$$y_+ = -0.032 \pm 0.048^{+0.010}_{-0.009} \pm 0.008,$$

where in each case the first uncertainty is statistical, the second systematic and the third is due to the choice of amplitude model used to describe the $D \to K^0_S\pi^+\pi^-$ decay. The results place constraints on the magnitude of the ratio of the interfering $B^\pm$ decay amplitudes, the strong phase difference between them and the CKM angle γ, giving the values $r_B = 0.06 \pm 0.04$, $\delta_B = (115^{+41}_{-51})^\circ$ and $\gamma = (84^{+49}_{-42})^\circ$. Neutral D meson mixing has a negligible effect on the parameters r_B, δ_B and γ.

These results are consistent with, complementary to, and cannot be combined with, those obtained by the LHCb model-independent analysis of the same data set [9]. The results are also consistent with world average values [34,35].

Acknowledgements

We express our gratitude to our colleagues in the CERN accelerator departments for the excellent performance of the LHC. We thank the technical and administrative staff at the LHCb institutes. We acknowledge support from CERN and from the national agencies: CAPES, CNPq, FAPERJ and FINEP (Brazil); NSFC (China); CNRS/IN2P3 (France); BMBF, DFG, HGF and MPG (Germany); SFI (Ireland); INFN (Italy); FOM and NWO (The Netherlands); MNiSW and NCN (Poland); MEN/IFA (Romania); MinES and FANO (Russia); MinECo (Spain); SNSF and SER (Switzerland); NASU (Ukraine); STFC (United Kingdom); NSF (USA). The Tier1 computing centres are supported by IN2P3 (France), KIT and BMBF (Germany), INFN (Italy), NWO and SURF (The Netherlands), PIC (Spain), GridPP (United Kingdom). We are indebted to the communities behind the multiple open source software packages on which we depend. We are also thankful for the computing resources and the access to software R&D tools provided by Yandex LLC (Russia). Individual groups or members have received support from EPLANET, Marie Skłodowska-Curie Actions and ERC (European Union), Conseil général de Haute-Savoie, Labex ENIGMASS and OCEVU, Région Auvergne (France), RFBR (Russia), XuntaGal and GENCAT (Spain), Royal Society and Royal Commission for the Exhibition of 1851 (United Kingdom).

References

[1] A. Giri, Y. Grossman, A. Soffer, J. Zupan, Determining γ using $B^\pm \to DK^\pm$ with multibody D decays, Phys. Rev. D 68 (2003) 054018, arXiv:hep-ph/0303187.

[2] A. Bondar, Proceedings of BINP special analysis meeting on Dalitz analysis, 24–26 Sep. 2002, unpublished.

[3] BaBar Collaboration, B. Aubert, et al., Measurement of the Cabibbo–Kobayashi–Maskawa angle γ in $B^\mp \to D^{(*)}K^\mp$ decays with a Dalitz analysis of $D \to K^0_S\pi^-\pi^+$, Phys. Rev. Lett. 95 (2005) 121802, arXiv:hep-ex/0504039.

[4] BaBar Collaboration, B. Aubert, et al., Improved measurement of the CKM angle γ in $B^\mp \to D^{(*)}K^{(*)\mp}$ decays with a Dalitz plot analysis of D decays to $K^0_S\pi^+\pi^-$ and $K^0_S K^+K^-$, Phys. Rev. D 78 (2008) 034023, arXiv:0804.2089.

[5] BaBar Collaboration, P. del Amo Sanchez, et al., Evidence for direct CP violation in the measurement of the Cabibbo–Kobayashi–Maskawa angle γ with $B^\mp \to D^{(*)}K^{(*)\mp}$ decays, Phys. Rev. Lett. 105 (2010) 121801, arXiv:1005.1096.

[6] Belle Collaboration, A. Poluektov, et al., Measurement of ϕ_3 with Dalitz plot analysis of $B^\pm \to D^{(*)}K^\pm$ decay, Phys. Rev. D 70 (2004) 072003, arXiv:hep-ex/0406067.

[7] Belle Collaboration, A. Poluektov, et al., Measurement of ϕ_3 with a Dalitz plot analysis of $B^+ \to D^{(*)} K^{(*)+}$ decay, Phys. Rev. D 73 (2006) 112009, arXiv:hep-ex/0604054.
[8] Belle Collaboration, A. Poluektov, et al., Evidence for direct CP violation in the decay $B^\pm \to D^{(*)} K^\pm$, $D \to K^0_S \pi^+ \pi^-$ and measurement of the CKM phase ϕ_3, Phys. Rev. D 81 (2010) 112002, arXiv:1003.3360.
[9] LHCb Collaboration, R. Aaij, et al., A model-independent Dalitz plot analysis of $B^\pm \to D K^\pm$ with $D \to K^0_S h^+ h^-$ ($h = \pi, K$) decays and constraints on the CKM angle γ, Phys. Lett. B 718 (2012) 43, arXiv:1209.5869.
[10] Belle Collaboration, H. Aihara, et al., First measurement of ϕ_3 with a model-independent Dalitz plot analysis of $B^\pm \to D K^\pm$, $D \to K^0_S \pi^+ \pi^-$ decay, Phys. Rev. D 85 (2012) 112014, arXiv:1204.6561.
[11] CLEO Collaboration, J. Libby, et al., Model-independent determination of the strong-phase difference between D^0 and $\bar{D}^0 \to K^0_{S,L} h^+ h^-$ ($h = \pi, K$) and its impact on the measurement of the CKM angle γ/ϕ_3, Phys. Rev. D 82 (2010) 112006, arXiv:1010.2817.
[12] LHCb Collaboration, A.A. Alves Jr., et al., The LHCb detector at the LHC, J. Instrum. 3 (2008) S08005.
[13] M. Adinolfi, et al., Performance of the LHCb RICH detector at the LHC, Eur. Phys. J. C 73 (2013) 2431, arXiv:1211.6759.
[14] V.V. Gligorov, M. Williams, Efficient, reliable and fast high-level triggering using a bonsai boosted decision tree, J. Instrum. 8 (2013) P02013, arXiv:1210.6861.
[15] T. Sjöstrand, S. Mrenna, P. Skands, PYTHIA 6.4 physics and manual, J. High Energy Phys. 05 (2006) 026, arXiv:hep-ph/0603175.
[16] I. Belyaev, et al., Handling of the generation of primary events in GAUSS, the LHCb simulation framework, in: Nuclear Science Symposium Conference Record (NSS/MIC), IEEE, 2010, p. 1155.
[17] D.J. Lange, The EvtGen particle decay simulation package, Nucl. Instrum. Methods A 462 (2001) 152.
[18] P. Golonka, Z. Was, PHOTOS Monte Carlo: a precision tool for QED corrections in Z and W decays, Eur. Phys. J. C 45 (2006) 97, arXiv:hep-ph/0506026.
[19] Geant4 Collaboration, J. Allison, et al., Geant4 developments and applications, IEEE Trans. Nucl. Sci. 53 (2006) 270.
[20] Geant4 Collaboration, S. Agostinelli, et al., Geant4: a simulation toolkit, Nucl. Instrum. Methods A 506 (2003) 250.
[21] M. Clemencic, et al., The LHCb simulation application, GAUSS: design, evolution and experience, J. Phys. Conf. Ser. 331 (2011) 032023.
[22] Particle Data Group, J. Beringer, et al., Review of particle physics, Phys. Rev. D 86 (2012) 010001, and 2013 partial update for the 2014 edition.
[23] W.D. Hulsbergen, Decay chain fitting with a Kalman filter, Nucl. Instrum. Methods A 552 (2005) 566, arXiv:physics/0503191.
[24] T. Skwarnicki, A study of the radiative cascade transitions between the Upsilon-prime and Upsilon resonances, PhD thesis, Institute of Nuclear Physics, Krakow, 1986, DESY-F31-86-02.
[25] ARGUS Collaboration, H. Albrecht, et al., Search for hadronic $b \to u$ decays, Phys. Lett. B 241 (1990) 278.
[26] BaBar Collaboration, P. del Amo Sanchez, et al., Measurement of $D^0 - \bar{D}^0$ mixing parameters using $D^0 \to K^0_S \pi^+ \pi^-$ and $D^0 \to K^0_S K^+ K^-$ decays, Phys. Rev. Lett. 105 (2010) 081803, arXiv:1004.5053. For further details, see also Ref. [4];
D.A. Milanes, Measurement of $D^0 - \bar{D}^0$ mixing in the BaBar experiment, PhD thesis, University of Valencia, 2010;
N. Lopez-March, Measurement of the CKM phase γ with the BaBar experiment, PhD thesis, University of Valencia, 2010;
J. Garra Tico, Measurement of the neutral D meson mixing parameters at the BaBar experiment, PhD thesis, University of Barcelona, 2010.
[27] LHCb Collaboration, R. Aaij, et al., First observation of CP violation in the decays of B^0_s mesons, Phys. Rev. Lett. 110 (2013), arXiv:1304.6173.
[28] LHCb Collaboration, R. Aaij, et al., Measurement of the $D^\pm$ production asymmetry in 7 TeV pp collisions, Phys. Lett. B 718 (2012) 902, arXiv:1210.4112.
[29] V. Anisovich, A. Sarantsev, K-matrix analysis of the ($I J^{(PC)} = 00^{++}$)-wave in the mass region below 1900 MeV, Eur. Phys. J. A 16 (2003) 229, arXiv:hep-ph/0204328.
[30] E791 Collaboration, E. Aitala, et al., Dalitz plot analysis of the decay $D^+ \to K^- \pi^+ \pi^+$ and indication of a low-mass scalar $K\pi$ resonance, Phys. Rev. Lett. 89 (2002) 121801, arXiv:hep-ex/0204018.
[31] D. Aston, et al., A study of $K^- \pi^+$ scattering in the reaction $K^- p \to K^- \pi^+ n$ at 11 GeV/c, Nucl. Phys. B 296 (1988) 493.
[32] M. Rama, Effect of $D - \bar{D}$ mixing in the extraction of γ with $B^- \to D^0 K^-$ and $B^- \to D^0 \pi^-$ decays, Phys. Rev. D 89 (2014) 014021, arXiv:1307.4384.

[33] Heavy Flavor Averaging Group, Y. Amhis, et al., Averages of b-hadron, c-hadron, and τ-lepton properties as of early 2012, arXiv:1207.1158, updated results and figures available at http://www.slac.stanford.edu/xorg/hfag/.

[34] CKMfitter group, J. Charles, et al., CP violation and the CKM matrix: assessing the impact of the asymmetric B factories, Eur. Phys. J. C 41 (2005) 1, arXiv:hep-ph/0406184, updated results and figures available at http://ckmfitter.in2p3.fr.

[35] UTfit Collaboration, M. Bona, et al., Model-independent constraints on $\Delta F = 2$ operators and the scale of new physics, J. High Energy Phys. 03 (2008) 049, arXiv:0707.0636, updated results and figures available at http://www.utfit.org.

LHCb Collaboration

R. Aaij [41], B. Adeva [37], M. Adinolfi [46], A. Affolder [52], Z. Ajaltouni [5], J. Albrecht [9], F. Alessio [38], M. Alexander [51], S. Ali [41], G. Alkhazov [30], P. Alvarez Cartelle [37], A.A. Alves Jr [25,38], S. Amato [2], S. Amerio [22], Y. Amhis [7], L. An [3], L. Anderlini [17,g], J. Anderson [40], R. Andreassen [57], M. Andreotti [16,f], J.E. Andrews [58], R.B. Appleby [54], O. Aquines Gutierrez [10], F. Archilli [38], A. Artamonov [35], M. Artuso [59], E. Aslanides [6], G. Auriemma [25,n], M. Baalouch [5], S. Bachmann [11], J.J. Back [48], A. Badalov [36], V. Balagura [31], W. Baldini [16], R.J. Barlow [54], C. Barschel [38], S. Barsuk [7], W. Barter [47], V. Batozskaya [28], A. Bay [39], L. Beaucourt [4], J. Beddow [51], F. Bedeschi [23], I. Bediaga [1], S. Belogurov [31], K. Belous [35], I. Belyaev [31], E. Ben-Haim [8], G. Bencivenni [18], S. Benson [38], J. Benton [46], A. Berezhnoy [32], R. Bernet [40], M.-O. Bettler [47], M. van Beuzekom [41], A. Bien [11], S. Bifani [45], T. Bird [54], A. Bizzeti [17,i], P.M. Bjørnstad [54], T. Blake [48], F. Blanc [39], J. Blouw [10], S. Blusk [59], V. Bocci [25], A. Bondar [34], N. Bondar [30,38], W. Bonivento [15,38], S. Borghi [54], A. Borgia [59], M. Borsato [7], T.J.V. Bowcock [52], E. Bowen [40], C. Bozzi [16], T. Brambach [9], J. van den Brand [42], J. Bressieux [39], D. Brett [54], M. Britsch [10], T. Britton [59], J. Brodzicka [54], N.H. Brook [46], H. Brown [52], A. Bursche [40], G. Busetto [22,q], J. Buytaert [38], S. Cadeddu [15], R. Calabrese [16,f], M. Calvi [20,k], M. Calvo Gomez [36,o], A. Camboni [36], P. Campana [18,38], D. Campora Perez [38], A. Carbone [14,d], G. Carboni [24,l], R. Cardinale [19,38,j], A. Cardini [15], H. Carranza-Mejia [50], L. Carson [50], K. Carvalho Akiba [2], G. Casse [52], L. Cassina [20], L. Castillo Garcia [38], M. Cattaneo [38], Ch. Cauet [9], R. Cenci [58], M. Charles [8], Ph. Charpentier [38], S. Chen [54], S.-F. Cheung [55], N. Chiapolini [40], M. Chrzaszcz [40,26], K. Ciba [38], X. Cid Vidal [38], G. Ciezarek [53], P.E.L. Clarke [50], M. Clemencic [38], H.V. Cliff [47], J. Closier [38], V. Coco [38], J. Cogan [6], E. Cogneras [5], P. Collins [38], A. Comerma-Montells [11], A. Contu [15,38], A. Cook [46], M. Coombes [46], S. Coquereau [8], G. Corti [38], M. Corvo [16,f], I. Counts [56], B. Couturier [38], G.A. Cowan [50], D.C. Craik [48],

M. Cruz Torres [60], S. Cunliffe [53], R. Currie [50], C. D'Ambrosio [38], J. Dalseno [46], P. David [8], P.N.Y. David [41], A. Davis [57], K. De Bruyn [41], S. De Capua [54], M. De Cian [11], J.M. De Miranda [1], L. De Paula [2], W. De Silva [57], P. De Simone [18], D. Decamp [4], M. Deckenhoff [9], L. Del Buono [8], N. Déléage [4], D. Derkach [55], O. Deschamps [5], F. Dettori [42], A. Di Canto [38], H. Dijkstra [38], S. Donleavy [52], F. Dordei [11], M. Dorigo [39], A. Dosil Suárez [37], D. Dossett [48], A. Dovbnya [43], G. Dujany [54], F. Dupertuis [39], P. Durante [38], R. Dzhelyadin [35], A. Dziurda [26], A. Dzyuba [30], S. Easo [49,38], U. Egede [53], V. Egorychev [31], S. Eidelman [34], S. Eisenhardt [50], U. Eitschberger [9], R. Ekelhof [9], L. Eklund [51,38], I. El Rifai [5], Ch. Elsasser [40], S. Ely [59], S. Esen [11], A. Falabella [16,f], C. Färber [11], C. Farinelli [41], N. Farley [45], S. Farry [52], R.F. Fay [52], D. Ferguson [50], V. Fernandez Albor [37], F. Ferreira Rodrigues [1], M. Ferro-Luzzi [38], S. Filippov [33], M. Fiore [16,f], M. Fiorini [16,f], M. Firlej [27], C. Fitzpatrick [38], T. Fiutowski [27], M. Fontana [10], F. Fontanelli [19,j], R. Forty [38], O. Francisco [2], M. Frank [38], C. Frei [38], M. Frosini [17,38,g], J. Fu [21,38], E. Furfaro [24,l], A. Gallas Torreira [37], D. Galli [14,d], S. Gallorini [22], S. Gambetta [19,j], M. Gandelman [2], P. Gandini [59], Y. Gao [3], J. Garofoli [59], J. Garra Tico [47,*], L. Garrido [36], C. Gaspar [38], R. Gauld [55], L. Gavardi [9], A. Geraci [21,u], E. Gersabeck [11], M. Gersabeck [54], T. Gershon [48], Ph. Ghez [4], A. Gianelle [22], S. Giani' [39], V. Gibson [47], L. Giubega [29], V.V. Gligorov [38], C. Göbel [60], D. Golubkov [31], A. Golutvin [53,31,38], A. Gomes [1,a], H. Gordon [38], C. Gotti [20], M. Grabalosa Gándara [5], R. Graciani Diaz [36], L.A. Granado Cardoso [38], E. Graugés [36], G. Graziani [17], A. Grecu [29], E. Greening [55], S. Gregson [47], P. Griffith [45], L. Grillo [11], O. Grünberg [62], B. Gui [59], E. Gushchin [33], Yu. Guz [35,38], T. Gys [38], C. Hadjivasiliou [59], G. Haefeli [39], C. Haen [38], S.C. Haines [47,*], S. Hall [53], B. Hamilton [58], T. Hampson [46], X. Han [11], S. Hansmann-Menzemer [11], N. Harnew [55], S.T. Harnew [46], J. Harrison [54], T. Hartmann [62], J. He [38], T. Head [38], V. Heijne [41], K. Hennessy [52], P. Henrard [5], L. Henry [8], J.A. Hernando Morata [37], E. van Herwijnen [38], M. Heß [62], A. Hicheur [1], D. Hill [55], M. Hoballah [5], C. Hombach [54], W. Hulsbergen [41], P. Hunt [55], N. Hussain [55], D. Hutchcroft [52], D. Hynds [51], M. Idzik [27], P. Ilten [56], R. Jacobsson [38], A. Jaeger [11], J. Jalocha [55], E. Jans [41], P. Jaton [39], A. Jawahery [58], F. Jing [3], M. John [55], D. Johnson [55], C.R. Jones [47], C. Joram [38], B. Jost [38], N. Jurik [59], M. Kaballo [9], S. Kandybei [43], W. Kanso [6], M. Karacson [38], T.M. Karbach [38], M. Kelsey [59],

I.R. Kenyon [45], T. Ketel [42], B. Khanji [20], C. Khurewathanakul [39], S. Klaver [54], O. Kochebina [7], M. Kolpin [11], I. Komarov [39], R.F. Koopman [42], P. Koppenburg [41,38], M. Korolev [32], A. Kozlinskiy [41], L. Kravchuk [33], K. Kreplin [11], M. Kreps [48], G. Krocker [11], P. Krokovny [34], F. Kruse [9], M. Kucharczyk [20,26,38,k], V. Kudryavtsev [34], K. Kurek [28], T. Kvaratskheliya [31], V.N. La Thi [39], D. Lacarrere [38], G. Lafferty [54], A. Lai [15], D. Lambert [50], R.W. Lambert [42], E. Lanciotti [38], G. Lanfranchi [18], C. Langenbruch [38], B. Langhans [38], T. Latham [48], C. Lazzeroni [45], R. Le Gac [6], J. van Leerdam [41], J.-P. Lees [4], R. Lefèvre [5], A. Leflat [32], J. Lefrançois [7], S. Leo [23], O. Leroy [6], T. Lesiak [26], B. Leverington [11], Y. Li [3], M. Liles [52], R. Lindner [38], C. Linn [38], F. Lionetto [40], B. Liu [15], G. Liu [38], S. Lohn [38], I. Longstaff [51], J.H. Lopes [2], N. Lopez-March [39], P. Lowdon [40], H. Lu [3], D. Lucchesi [22,q], H. Luo [50], A. Lupato [22], E. Luppi [16,f], O. Lupton [55], F. Machefert [7], I.V. Machikhiliyan [31], F. Maciuc [29], O. Maev [30], S. Malde [55], G. Manca [15,e], G. Mancinelli [6], A. Mapelli [38], J. Maratas [5], J.F. Marchand [4], U. Marconi [14], C. Marin Benito [36], P. Marino [23,s], R. Märki [39], J. Marks [11], G. Martellotti [25], A. Martens [8], A. Martín Sánchez [7], M. Martinelli [41], D. Martinez Santos [42], F. Martinez Vidal [64], D. Martins Tostes [2], A. Massafferri [1], R. Matev [38], Z. Mathe [38], C. Matteuzzi [20], A. Mazurov [16,f], M. McCann [53], J. McCarthy [45], A. McNab [54], R. McNulty [12], B. McSkelly [52], B. Meadows [57,55], F. Meier [9], M. Meissner [11], M. Merk [41], D.A. Milanes [8], M.-N. Minard [4], N. Moggi [14], J. Molina Rodriguez [60], S. Monteil [5], D. Moran [54], M. Morandin [22], P. Morawski [26], A. Mordà [6], M.J. Morello [23,s], J. Moron [27], A.-B. Morris [50], R. Mountain [59], F. Muheim [50], K. Müller [40], R. Muresan [29], M. Mussini [14], B. Muster [39], P. Naik [46], T. Nakada [39], R. Nandakumar [49], I. Nasteva [2], M. Needham [50], N. Neri [21], S. Neubert [38], N. Neufeld [38], M. Neuner [11], A.D. Nguyen [39], T.D. Nguyen [39], C. Nguyen-Mau [39,p], M. Nicol [7], V. Niess [5], R. Niet [9], N. Nikitin [32], T. Nikodem [11], A. Novoselov [35], A. Oblakowska-Mucha [27], V. Obraztsov [35], S. Oggero [41], S. Ogilvy [51], O. Okhrimenko [44], R. Oldeman [15,e], G. Onderwater [65], M. Orlandea [29], J.M. Otalora Goicochea [2], P. Owen [53], A. Oyanguren [64], B.K. Pal [59], A. Palano [13,c], F. Palombo [21,t], M. Palutan [18], J. Panman [38], A. Papanestis [49,38], M. Pappagallo [51], C. Parkes [54], C.J. Parkinson [9,45], G. Passaleva [17], G.D. Patel [52], M. Patel [53], C. Patrignani [19,j], A. Pazos Alvarez [37], A. Pearce [54], A. Pellegrino [41], M. Pepe Altarelli [38],

S. Perazzini [14,d], E. Perez Trigo [37], P. Perret [5], M. Perrin-Terrin [6], L. Pescatore [45], E. Pesen [66], K. Petridis [53], A. Petrolini [19,j], E. Picatoste Olloqui [36], B. Pietrzyk [4], T. Pilař [48], D. Pinci [25], A. Pistone [19], S. Playfer [50], M. Plo Casasus [37], F. Polci [8], A. Poluektov [48,34], E. Polycarpo [2], A. Popov [35], D. Popov [10], B. Popovici [29], C. Potterat [2], A. Powell [55], J. Prisciandaro [39], A. Pritchard [52], C. Prouve [46], V. Pugatch [44], A. Puig Navarro [39], G. Punzi [23,r], W. Qian [4], B. Rachwal [26], J.H. Rademacker [46], B. Rakotomiaramanana [39], M. Rama [18], M.S. Rangel [2], I. Raniuk [43], N. Rauschmayr [38], G. Raven [42], S. Reichert [54], M.M. Reid [48], A.C. dos Reis [1], S. Ricciardi [49], A. Richards [53], M. Rihl [38], K. Rinnert [52], V. Rives Molina [36], D.A. Roa Romero [5], P. Robbe [7], A.B. Rodrigues [1], E. Rodrigues [54], P. Rodriguez Perez [54], S. Roiser [38], V. Romanovsky [35], A. Romero Vidal [37], M. Rotondo [22], J. Rouvinet [39], T. Ruf [38], F. Ruffini [23], H. Ruiz [36], P. Ruiz Valls [64], G. Sabatino [25,l], J.J. Saborido Silva [37], N. Sagidova [30], P. Sail [51], B. Saitta [15,e], V. Salustino Guimaraes [2], C. Sanchez Mayordomo [64], B. Sanmartin Sedes [37], R. Santacesaria [25], C. Santamarina Rios [37], E. Santovetti [24,l], M. Sapunov [6], A. Sarti [18,m], C. Satriano [25,n], A. Satta [24], M. Savrie [16,f], D. Savrina [31,32], M. Schiller [42], H. Schindler [38], M. Schlupp [9], M. Schmelling [10], B. Schmidt [38], O. Schneider [39], A. Schopper [38], M.-H. Schune [7], R. Schwemmer [38], B. Sciascia [18], A. Sciubba [25], M. Seco [37], A. Semennikov [31], K. Senderowska [27], I. Sepp [53], N. Serra [40], J. Serrano [6], L. Sestini [22], P. Seyfert [11], M. Shapkin [35], I. Shapoval [16,43,f], Y. Shcheglov [30], T. Shears [52], L. Shekhtman [34], V. Shevchenko [63], A. Shires [9], R. Silva Coutinho [48], G. Simi [22], M. Sirendi [47], N. Skidmore [46], T. Skwarnicki [59], N.A. Smith [52], E. Smith [55,49], E. Smith [53], J. Smith [47], M. Smith [54], H. Snoek [41], M.D. Sokoloff [57], F.J.P. Soler [51], F. Soomro [39], D. Souza [46], B. Souza De Paula [2], B. Spaan [9], A. Sparkes [50], P. Spradlin [51], F. Stagni [38], S. Stahl [11], O. Steinkamp [40], O. Stenyakin [35], S. Stevenson [55], S. Stoica [29], S. Stone [59], B. Storaci [40], S. Stracka [23,38], M. Straticiuc [29], U. Straumann [40], R. Stroili [22], V.K. Subbiah [38], L. Sun [57], W. Sutcliffe [53], K. Swientek [27], S. Swientek [9], V. Syropoulos [42], M. Szczekowski [28], P. Szczypka [39,38], D. Szilard [2], T. Szumlak [27], S. T'Jampens [4], M. Teklishyn [7], G. Tellarini [16,f], F. Teubert [38], C. Thomas [55], E. Thomas [38], J. van Tilburg [41], V. Tisserand [4], M. Tobin [39], S. Tolk [42], L. Tomassetti [16,f], D. Tonelli [38], S. Topp-Joergensen [55], N. Torr [55], E. Tournefier [4], S. Tourneur [39],

M.T. Tran [39], M. Tresch [40], A. Tsaregorodtsev [6], P. Tsopelas [41], N. Tuning [41], M. Ubeda Garcia [38], A. Ukleja [28], A. Ustyuzhanin [63], U. Uwer [11], V. Vagnoni [14], G. Valenti [14], A. Vallier [7], R. Vazquez Gomez [18], P. Vazquez Regueiro [37], C. Vázquez Sierra [37], S. Vecchi [16], J.J. Velthuis [46], M. Veltri [17,h], G. Veneziano [39], M. Vesterinen [11], B. Viaud [7], D. Vieira [2], M. Vieites Diaz [37], X. Vilasis-Cardona [36,o], A. Vollhardt [40], D. Volyanskyy [10], D. Voong [46], A. Vorobyev [30], V. Vorobyev [34], C. Voß [62], H. Voss [10], J.A. de Vries [41], R. Waldi [62], C. Wallace [48], R. Wallace [12], J. Walsh [23], S. Wandernoth [11], J. Wang [59], D.R. Ward [47], N.K. Watson [45], D. Websdale [53], M. Whitehead [48], J. Wicht [38], D. Wiedner [11], G. Wilkinson [55], M.P. Williams [45], M. Williams [56], F.F. Wilson [49], J. Wimberley [58], J. Wishahi [9], W. Wislicki [28], M. Witek [26], G. Wormser [7], S.A. Wotton [47], S. Wright [47], S. Wu [3], K. Wyllie [38], Y. Xie [61], Z. Xing [59], Z. Xu [39], Z. Yang [3], X. Yuan [3], O. Yushchenko [35], M. Zangoli [14], M. Zavertyaev [10,b], F. Zhang [3], L. Zhang [59], W.C. Zhang [12], Y. Zhang [3], A. Zhelezov [11], A. Zhokhov [31], L. Zhong [3], A. Zvyagin [38]

[1] *Centro Brasileiro de Pesquisas Físicas (CBPF), Rio de Janeiro, Brazil*
[2] *Universidade Federal do Rio de Janeiro (UFRJ), Rio de Janeiro, Brazil*
[3] *Center for High Energy Physics, Tsinghua University, Beijing, China*
[4] *LAPP, Université de Savoie, CNRS/IN2P3, Annecy-Le-Vieux, France*
[5] *Clermont Université, Université Blaise Pascal, CNRS/IN2P3, LPC, Clermont-Ferrand, France*
[6] *CPPM, Aix-Marseille Université, CNRS/IN2P3, Marseille, France*
[7] *LAL, Université Paris-Sud, CNRS/IN2P3, Orsay, France*
[8] *LPNHE, Université Pierre et Marie Curie, Université Paris Diderot, CNRS/IN2P3, Paris, France*
[9] *Fakultät Physik, Technische Universität Dortmund, Dortmund, Germany*
[10] *Max-Planck-Institut für Kernphysik (MPIK), Heidelberg, Germany*
[11] *Physikalisches Institut, Ruprecht-Karls-Universität Heidelberg, Heidelberg, Germany*
[12] *School of Physics, University College Dublin, Dublin, Ireland*
[13] *Sezione INFN di Bari, Bari, Italy*
[14] *Sezione INFN di Bologna, Bologna, Italy*
[15] *Sezione INFN di Cagliari, Cagliari, Italy*
[16] *Sezione INFN di Ferrara, Ferrara, Italy*
[17] *Sezione INFN di Firenze, Firenze, Italy*
[18] *Laboratori Nazionali dell'INFN di Frascati, Frascati, Italy*
[19] *Sezione INFN di Genova, Genova, Italy*
[20] *Sezione INFN di Milano Bicocca, Milano, Italy*
[21] *Sezione INFN di Milano, Milano, Italy*
[22] *Sezione INFN di Padova, Padova, Italy*
[23] *Sezione INFN di Pisa, Pisa, Italy*
[24] *Sezione INFN di Roma Tor Vergata, Roma, Italy*
[25] *Sezione INFN di Roma La Sapienza, Roma, Italy*
[26] *Henryk Niewodniczanski Institute of Nuclear Physics Polish Academy of Sciences, Kraków, Poland*
[27] *AGH – University of Science and Technology, Faculty of Physics and Applied Computer Science, Kraków, Poland*
[28] *National Center for Nuclear Research (NCBJ), Warsaw, Poland*
[29] *Horia Hulubei National Institute of Physics and Nuclear Engineering, Bucharest-Magurele, Romania*
[30] *Petersburg Nuclear Physics Institute (PNPI), Gatchina, Russia*
[31] *Institute of Theoretical and Experimental Physics (ITEP), Moscow, Russia*

[32] *Institute of Nuclear Physics, Moscow State University (SINP MSU), Moscow, Russia*
[33] *Institute for Nuclear Research of the Russian Academy of Sciences (INR RAN), Moscow, Russia*
[34] *Budker Institute of Nuclear Physics (SB RAS) and Novosibirsk State University, Novosibirsk, Russia*
[35] *Institute for High Energy Physics (IHEP), Protvino, Russia*
[36] *Universitat de Barcelona, Barcelona, Spain*
[37] *Universidad de Santiago de Compostela, Santiago de Compostela, Spain*
[38] *European Organization for Nuclear Research (CERN), Geneva, Switzerland*
[39] *Ecole Polytechnique Fédérale de Lausanne (EPFL), Lausanne, Switzerland*
[40] *Physik-Institut, Universität Zürich, Zürich, Switzerland*
[41] *Nikhef National Institute for Subatomic Physics, Amsterdam, The Netherlands*
[42] *Nikhef National Institute for Subatomic Physics and VU University Amsterdam, Amsterdam, The Netherlands*
[43] *NSC Kharkiv Institute of Physics and Technology (NSC KIPT), Kharkiv, Ukraine*
[44] *Institute for Nuclear Research of the National Academy of Sciences (KINR), Kyiv, Ukraine*
[45] *University of Birmingham, Birmingham, United Kingdom*
[46] *H.H. Wills Physics Laboratory, University of Bristol, Bristol, United Kingdom*
[47] *Cavendish Laboratory, University of Cambridge, Cambridge, United Kingdom*
[48] *Department of Physics, University of Warwick, Coventry, United Kingdom*
[49] *STFC Rutherford Appleton Laboratory, Didcot, United Kingdom*
[50] *School of Physics and Astronomy, University of Edinburgh, Edinburgh, United Kingdom*
[51] *School of Physics and Astronomy, University of Glasgow, Glasgow, United Kingdom*
[52] *Oliver Lodge Laboratory, University of Liverpool, Liverpool, United Kingdom*
[53] *Imperial College London, London, United Kingdom*
[54] *School of Physics and Astronomy, University of Manchester, Manchester, United Kingdom*
[55] *Department of Physics, University of Oxford, Oxford, United Kingdom*
[56] *Massachusetts Institute of Technology, Cambridge, MA, United States*
[57] *University of Cincinnati, Cincinnati, OH, United States*
[58] *University of Maryland, College Park, MD, United States*
[59] *Syracuse University, Syracuse, NY, United States*
[60] *Pontifícia Universidade Católica do Rio de Janeiro (PUC-Rio), Rio de Janeiro, Brazil* [v]
[61] *Institute of Particle Physics, Central China Normal University, Wuhan, Hubei, China* [w]
[62] *Institut für Physik, Universität Rostock, Rostock, Germany* [x]
[63] *National Research Centre Kurchatov Institute, Moscow, Russia, associated to* [y]
[64] *Instituto de Fisica Corpuscular (IFIC), Universitat de Valencia-CSIC, Valencia, Spain* [z]
[65] *KVI – University of Groningen, Groningen, The Netherlands* [aa]
[66] *Celal Bayar University, Manisa, Turkey* [ab]

[*] Corresponding authors.
[a] Universidade Federal do Triângulo Mineiro (UFTM), Uberaba-MG, Brazil.
[b] P.N. Lebedev Physical Institute, Russian Academy of Science (LPI RAS), Moscow, Russia.
[c] Università di Bari, Bari, Italy.
[d] Università di Bologna, Bologna, Italy.
[e] Università di Cagliari, Cagliari, Italy.
[f] Università di Ferrara, Ferrara, Italy.
[g] Università di Firenze, Firenze, Italy.
[h] Università di Urbino, Urbino, Italy.
[i] Università di Modena e Reggio Emilia, Modena, Italy.
[j] Università di Genova, Genova, Italy.
[k] Università di Milano Bicocca, Milano, Italy.
[l] Università di Roma Tor Vergata, Roma, Italy.
[m] Università di Roma La Sapienza, Roma, Italy.
[n] Università della Basilicata, Potenza, Italy.
[o] LIFAELS, La Salle, Universitat Ramon Llull, Barcelona, Spain.
[p] Hanoi University of Science, Hanoi, Viet Nam.
[q] Università di Padova, Padova, Italy.

[r] Università di Pisa, Pisa, Italy.
[s] Scuola Normale Superiore, Pisa, Italy.
[t] Università degli Studi di Milano, Milano, Italy.
[u] Politecnico di Milano, Milano, Italy.
[v] Associated to Universidade Federal do Rio de Janeiro (UFRJ), Rio de Janeiro, Brazil.
[w] Associated to Center for High Energy Physics, Tsinghua University, Beijing, China.
[x] Associated to Physikalisches Institut, Ruprecht-Karls-Universität Heidelberg, Heidelberg, Germany.
[y] Associated to Institute of Theoretical and Experimental Physics (ITEP), Moscow, Russia.
[z] Associated to Universitat de Barcelona, Barcelona, Spain.
[aa] Associated to Nikhef National Institute for Subatomic Physics, Amsterdam, The Netherlands.
[ab] Associated to European Organization for Nuclear Research (CERN), Geneva, Switzerland.